Long-Term Stability Test System for High-Voltage, High-Frequency SiC Power Devices

Tam H. Duong[1,2], David W. Berning[2], A. R. Hefner, Jr. [2], Keyue M. Smedley[1]

[1]Dept. of Electrical Engineering and Computer Science
University of California, Irvine
Irvine, CA 92697

[2]National Institute of Standards and Technology
Semiconductor Electronics Division
Gaithersburg, MD 20899

***Abstract*-This paper presents a test system developed for long-term stability characterization of 10 kV Silicon Carbide (SiC) power MOSFETs and SiC diodes under 20 kHz hard switching conditions. The system is designed to test a single power switch and a single power diode for continuous or burst switching conditions up to 5 kV and 5 A. The test system includes a 4.5 kV to 5 kV boost converter to emulate a 22.5 kW hard switching power converter. An additional DC-DC converter is used to recover the power processed by the boost converter. The design criteria, simulation, and construction of the test system are discussed in this paper and the system operation is demonstrated using various high voltage devices including 4.5 kV Silicon IGBTs, 10-kV SiC MOSFETs and 15 kV stacked silicon diodes.**

I. Introduction

Recent breakthroughs in Silicon Carbide (SiC) material and fabrication technology have led to the development of High-Voltage, High-Frequency (HV-HF) power devices with 10-kV, 20-kHz power switching capability [1, 2]. The emergence of HV-HF devices with such capability is expected to revolutionize commercial and military power distribution and conversion by extending the use of switch-mode power conversion to high voltage applications [3].

Currently, there are significant efforts underway to accelerate the development and application insertion of the new HV-HF SiC devices needed for commercial and military power conversion and distribution applications. The goal of the ongoing Defense Advanced Research Projects Agency (DARPA) Wide Band-gap Semiconductor Technology (WBST) High Power Electronics (HPE) program is to develop 10 kV, 100 A, 20 kHz class power semiconductor devices, therefore enabling future electric ships, more electric aircraft, and all electric combat vehicles [4, 5, 6]. DARPA is particularly interested in developing the power electronics device technology deemed necessary to enable a 2.7 MVA Solid State Power Substations (SSPS) for future Navy warships in the HPE Phase 3 program [7].

Although rapid advancement has been achieved for high voltage (>10 kV) SiC devices to date, long-term stability and reliability need to be demonstrated before SiC power devices can be utilized in system applications [8]. The purpose of this paper is to develop a power electronics test system to study the long-term stability of high voltage SiC power devices in switch mode power conversion applications. The test system operation is demonstrated using various high voltage devices including 4.5 kV Silicon IGBTs, 10-kV SiC MOSFETs and 15 kV stacked silicon diodes.

II. Test System Description

The diagram of the high voltage switch mode power conversion long-term reliability test system is shown in Fig.1 where (a) shows the basic boost converter indicating the switch and diode under test (Q_{DUT} and D_{DUT} respectively), (b) shows the input-ground-referenced high-voltage boost converter configuration used in this work, and (c) shows the power supply configuration for the ground-referenced boost converter. The boost converter is chosen because it enables testing a single switch and diode for hard switching conditions.

The input ground-referenced configuration enables the use of a relatively inexpensive 500 V commercial power supply for the power source, and the use of a 500 V to 4.5-kV voltage-multiplier-based power recovery converter that can be constructed using high efficiency semiconductor devices in the 500 V application range. Furthermore, the factor of nine voltage multiplication results in a 10 % duty cycle for the boost converter switch (Q_{DUT}) providing adequate time (5 us) to establish a fully-on condition for Q_{DUT}. The 10 % duty cycle also results in a recalculating power of only 2.25 kW while emulating a 22.5 kW hard-switched power converter.

1-4244-0714-1/07/$20.00 ©2007 IEEE.

A. High Voltage Boost Converter Test Circuit

The input-ground-referenced high-voltage boost converter of Fig.1 is designed to operate in a continuous conduction mode (CCM) at 20-kHz switching frequency with duty cycle (D) of 10%. To achieve D=10% while having the output voltage (V_{OUT}) of the boost converter to be 5000 V, the input voltage (V_{IN}) must be 4500 V because (1-D) ≈ V_{IN}/V_{OUT} for the boost converter. Due to the input ground-referenced configuration, the source of Q_{DUT} is at -4.5 kV and a high-voltage isolated gate-drive transformer is required. A burst operation mode is also included to provide the capability to test the devices at the full current and voltage level, but with lower average power loss and cooling requirements than continuous mode operation. On the other hand, the continuous operation mode results in more switching cycles in a shorter period of time, and thus accelerates the long-term switching stress reliability testing.

B. Power Recovery DC-DC Converter

The -4.5 kV power recovery DC-DC converter consists of a ten-stage voltage multiplier circuit as shown in Fig. 2 and an input half-bridge as shown in Fig. 3. The power recovery circuit converts a 500 VDC source (V_S) to a -4500 VDC output (V_C) as shown Fig. 1c where ten stages are used instead of nine to provide additional power supply voltage margin. The output voltage between nodes C and GND, called V_{C_GND}, is ideally equal to $-2nV_{B\_GNDpeak}$, where n is the number of stages in the multiplier. To achieve high efficiency, the input half bridge uses COOLMOS* transistors and the voltage multiplier uses 600 V ultra fast soft recovery diodes and high-current polypropylene film type capacitors. The measured efficiency of the power recovery circuit is 97 % at full power.

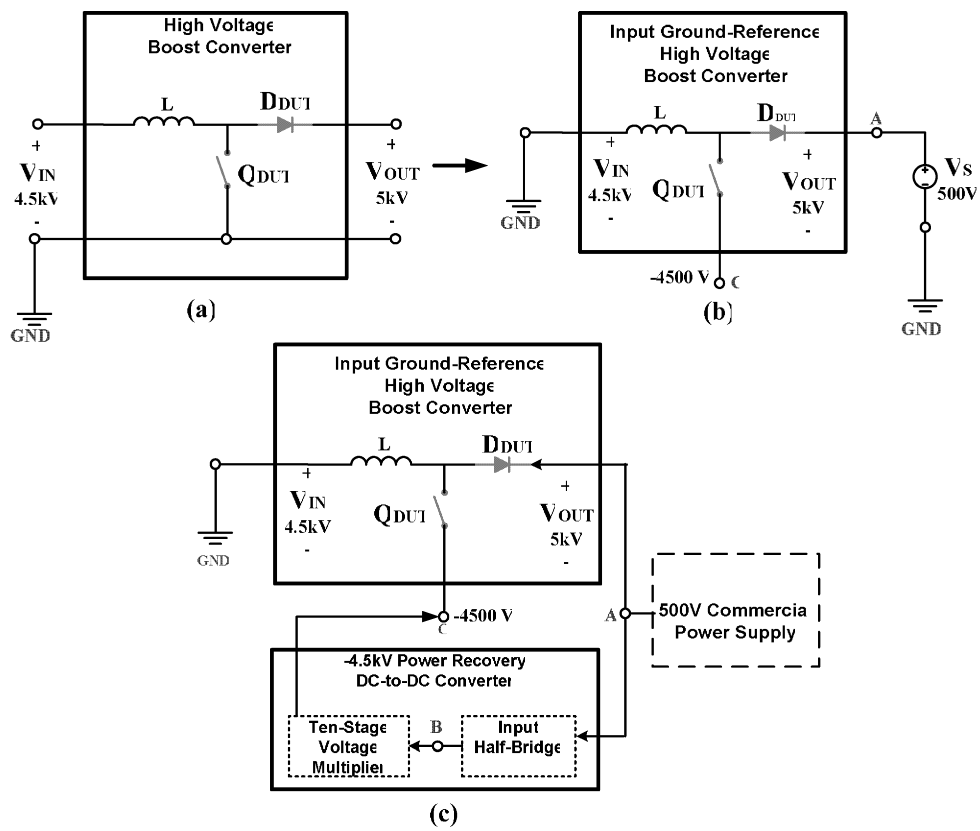

Fig. 1: Diagram of the high voltage switch mode power conversion long-term reliability test system: (a) the basic boost converter indicating the switch and diode under test (Q_{DUT} and D_{DUT} respectively), (b) the input ground-referenced high voltage boost converter configuration used in this work, and (c) the power supply configuration for the ground referenced boost converter.

* COOMOS is a trademark of Infineon Inc. Certain commercial products are identified to better describe procedures used in this work. This identification does not constitute endorsement of these products by NIST, or the implication that the identified products are necessarily the best for the purpose.

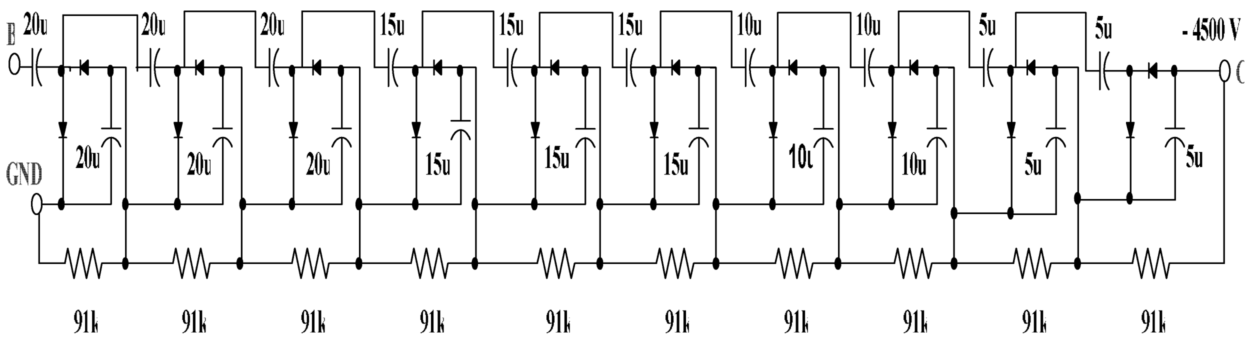

Fig. 2: Circuit diagram of the ten-stage voltage multiplier block in Fig. 1c.

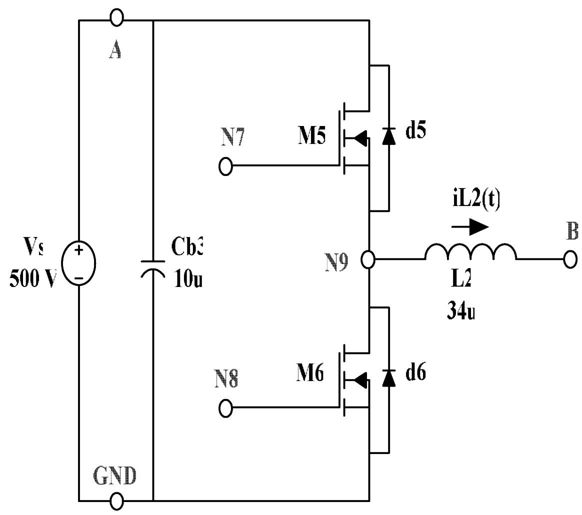

Fig. 3: Circuit diagram of the input half-bridge for the 500 V to -4.5 kV recirculating power converter.

C. Windowing Circuit for Measuring On-state Voltage

Since the on-state voltage of SiC power MOSFETs is a temperature sensitive parameter, it can be used to measure and monitor temperature during the test system operation. However, a 1000 X probe must be used to measure the drain-source voltage (V_{DS}) because it rises to 5 kV when the device is switched off and 1000 X probes can not resolve the small changes in on-state voltage with temperature. Therefore, the windowing circuit shown in Fig. 4 is used to isolate the on-state voltage measurement circuit from the high voltage V_{DS} that occurs during the off-state and switching.

The windowing circuit operates synchronously with the gate drive of the boost converter circuit so that the on-state voltage measurement circuit is connected to V_{DS} only during the time that Q_{DUT} is ON, and is isolated from V_{DS} when Q_{DUT} is OFF or being switched. Due to the presence of 5 kV transitions, a high voltage vacuum tube triode (6BK4C) [9] is used as the switch to either pass the signal or isolate V_{DS} from the holding capacitor at the input of the on-state voltage measurement circuit. The holding capacitor acts to sample-and-hold the on-state voltage measured from the repetitive samplings of the V_{DS} signal during the ON period. The voltage on the holding capacitor is buffered and transformed to a ground-referenced voltage signal needed for the oscilloscope using a high-frequency-modulated transformer isolation circuit.

The components on the left hand side of Fig. 4 form the gating signal for the vacuum tube triode and determine the on-state voltage measurement window. This tube gating signal is coupled through the top isolation transformer (T5) to the tube grid. The timing signal logic is implemented using a dual monostable mutivibrator with Schmitt-Trigger inputs chip (SN74LS221) [10]. The dual monostable multivibrator incorporates adjustments to allow both the selection of the window width and its position relative to the ON interval of the Q_{DUT}.

The components on the bottom right-hand side of Fig. 4 are used to transform the signal on the holding capacitor to the ground-referenced voltage signal needed for the oscilloscope. The bottom transformer (T6) is used to couple a 20 kHz oscillator signal (N_O) to the gates of the MOSFETs (Q_2 and Q_3) just to the right of this transformer. These MOSFETs are used to generate the high-frequency-modulation of the holding capacitor signal. The transformer to the right of the MOSFETs (T7) isolates the high voltage from the ground referenced output signal section. The high-frequency modulated holding-capacitor signal is passed through this transformer and the high-frequency carrier signal is removed by the rectifier bridge composed of diodes D_7 to D_{10}. The output signal V_{out} is connected to a DVM that is read by the system monitoring software as described in section D. This signal is used to calculate the junction temperature of Q_{DUT}.

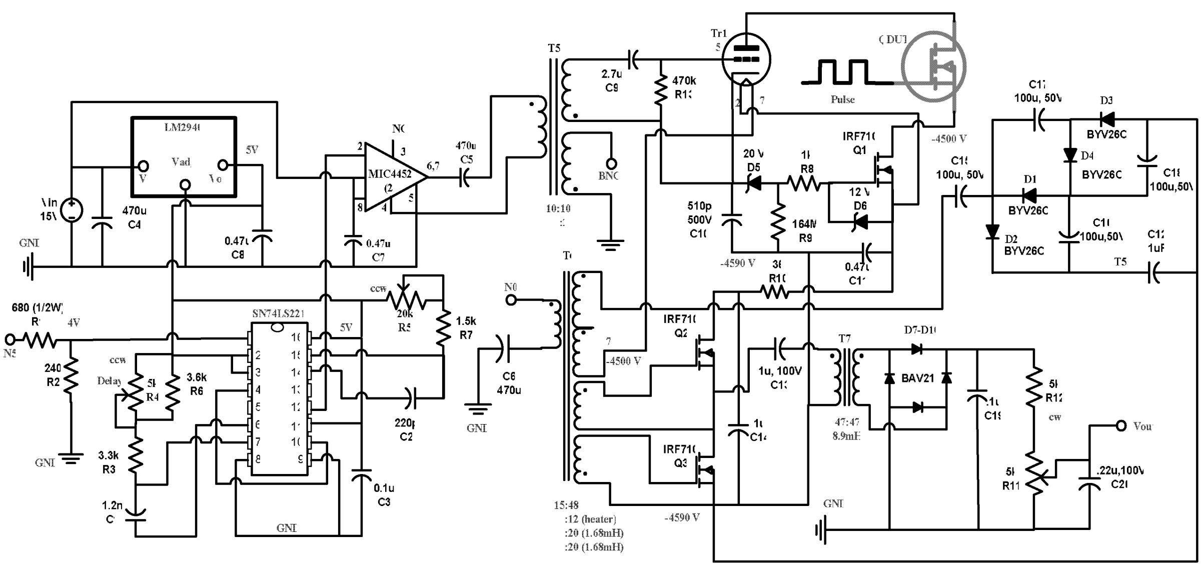

Fig. 4: Windowing circuit for measuring the on-state voltage of the SiC MOSFET (Q_{DUT}).

D. System User Interface and Monitoring

Fig. 5 shows the graphical user interface for the long-term switching stability test system and Fig. 6 shows the block diagram of the system indicating the instruments controlled by the computer. The computer-controlled instruments of Fig. 6 include a 500 V commercial source power supply, a pulse generator to implement burst mode operation, an oscilloscope to capture the switching waveforms, and a temperature controller to monitor the DUT heat sink. The test system control and monitoring software program monitors the heat sink temperature, junction temperature, and power supply current; and initiates a system shutdown when specified system parameters are exceeded. The program also periodically records stress time and monitors device characteristics to maintain a history of each device tested.

The control related parameters specified on the user interface of Fig. 5 are described as follows: The *Power Supply Control* is used to control and display the current values of the applied supply voltage and to limit the current drawn from the 500 V source power supply. The *Burst Control* is used to control the burst pulse width, the number of burst pulses, and the duty cycle for the burst pulses. The *Trigger Control* allows the user to determine which gate pulse within the burst pulse is to be measured. This selected gate pulse can be specified using a time delay from the beginning of each burst pulse or using the number of gate pulses after the beginning of each burst pulse. A function is also provided to trigger on the last gate pulse within the burst pulse.

The measurement related parameters specified on the user interface of Fig. 5 are described as follows: The *Measure Control* parameters are used to specify the range of the on-state pulse where I_{on} and V_{on} are to be averaged. The *Stop* and *Log* criteria parameters are used to specify the frequency for logging data and the criteria for stopping the test, as well as displaying the current value for the monitored parameters. The values monitored include the temperatures, power supply output, on-state voltage and current, and the number of cycles. The vertical slide bar control is used to specify the monitored parameters that are to be plotted in the graph on the upper right-hand side of Fig. 5.

The *Smooth Factor* horizontal slide bar control is used to define the data averaging for the measured waveforms shown in the two graphs at the bottom of Fig. 5. On the vertical axis of each graph, there is an option that allows the user to display or hide a particular waveform. The horizontal slide controls at the bottom of these graphs are used to zoom and position the measured waveforms.

Fig. 7 shows two pop-up panels that are accessible from the "Options" pull down menu located at the top of the user interface. Option (a) *Device Options* is used to set the maximum safe power supply voltage and duty cycle for the DUT, the MOSFET parameters (obtained from IMPACT tools [11]) used to calculate the junction temperature $T_{j(th)}$, from the on-state voltage, the thermal resistances used to calculate the junction temperature and device power dissipation from the measured heat sink and ambient temperatures. Option (b) *Circuit Options* is used to set up the maximum *Slew Rate* and *Mininum Step Voltage* for the source power supply to prevent overshoots in supply voltage.

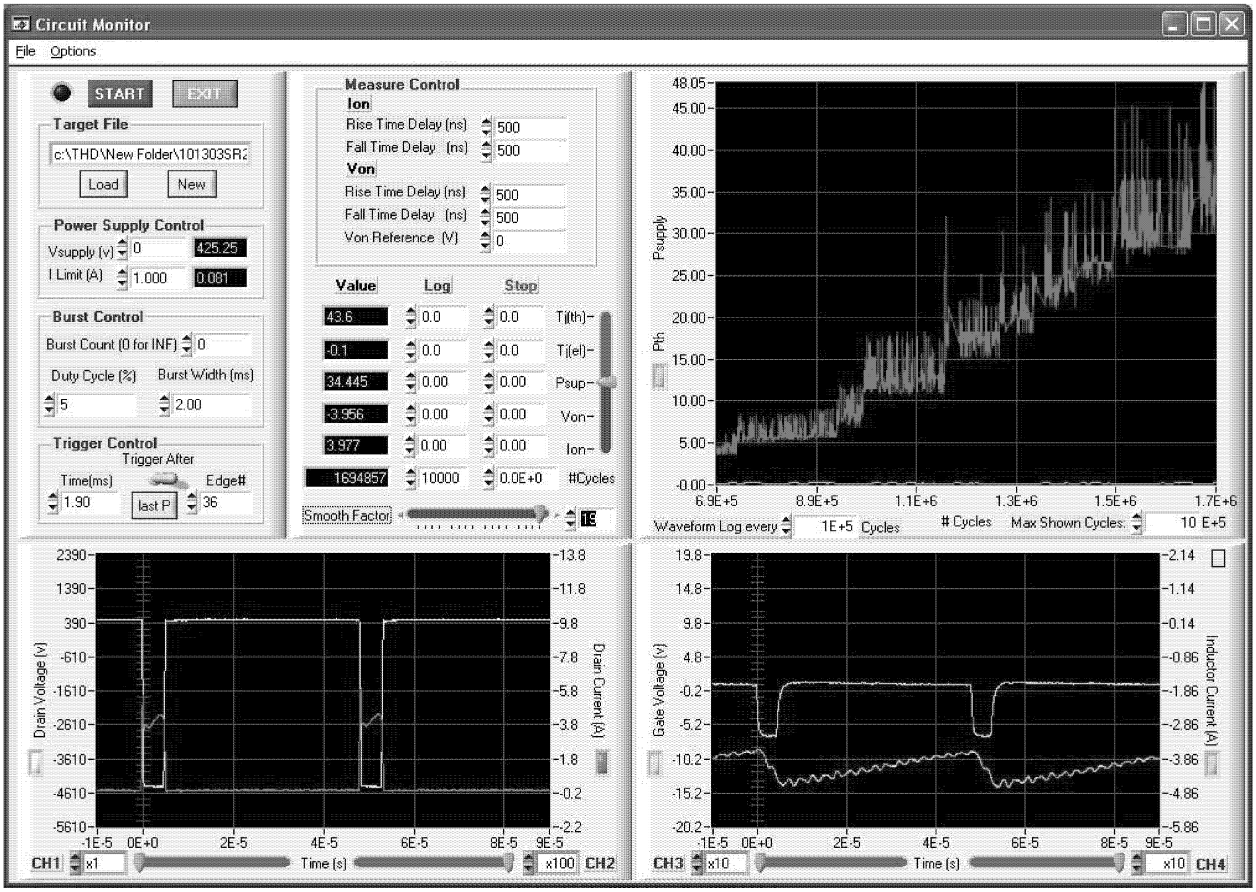

Fig. 5: Graphical user interface for the computer-controlled software tool used to control and monitor the high voltage long-term switching stability test system.

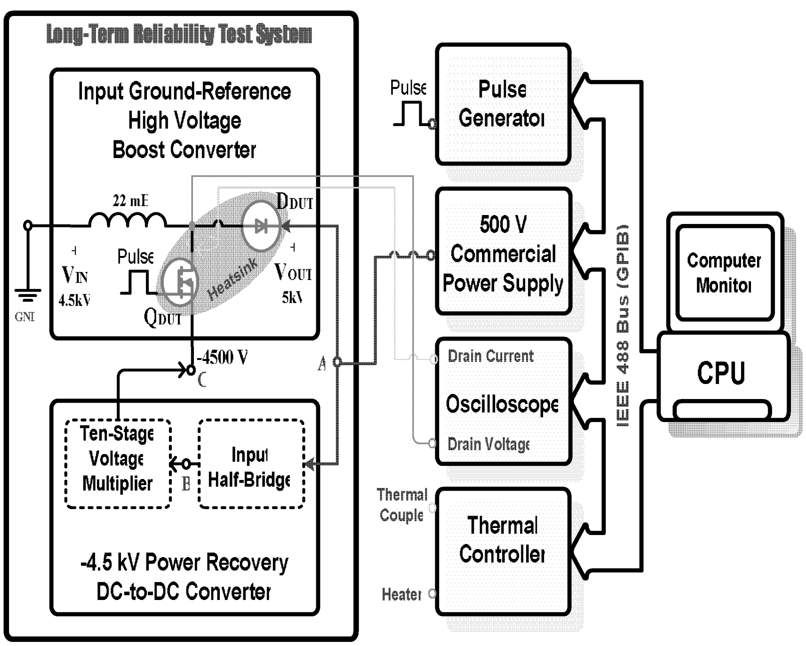

Fig. 6: Block diagram representation for the long-term reliability test system, including the computer-controlled instrumentation used to monitor and control it.

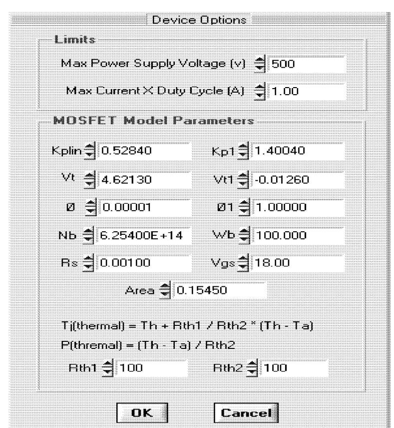

(a)

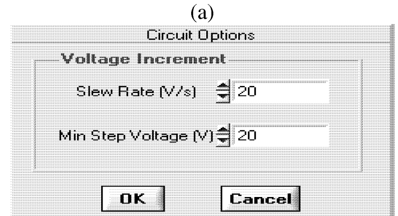

(b)

Fig. 7: Device and circuit options from the Options menu bar of Fig. 5.

III. MEASUREMENT RESULTS

Fig. 8 shows measured anode voltage, anode current, and inductor current waveforms from the long-term switching stability test using a 4.5 kV, 60 A Silicon IGBT as Q_{DUT} and Fig. 9 shows an expanded view of the Silicon IGBT waveforms. Figs. 10 and 11 show similar results using a 10 kV, 5 A SiC MOSFET as Q_{DUT}. The 4.5 kV Silicon IGBT waveforms were performed for a collector-emitter voltage of 2.8 kV to provide adequate voltage margin whereas the 10 kV SiC MOSFET measurement was performed for a drain-source voltage of 5 kV providing a large voltage margin. The 4.5 kV Silicon IGBT switching time is approximately 2 µs and the 10 kV SiC MOSFET switching time is approximately 100 ns; about 20 times faster than the Silicon IGBT.

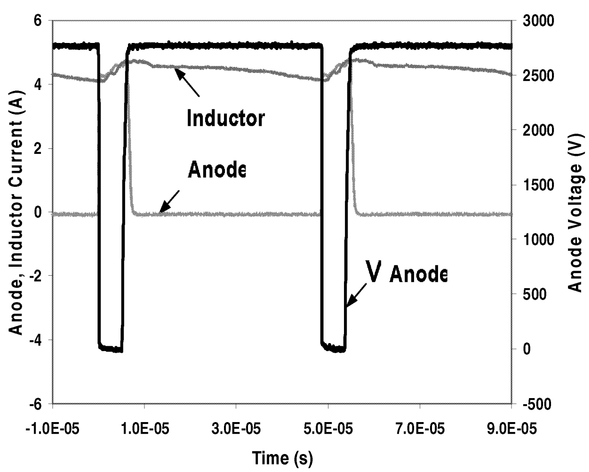

Fig.8: Measured anode voltage, anode current, and inductor current waveforms from the long-term switching stability test using a 4.5 kV, 60 A Silicon IGBT as Q_{DUT}.

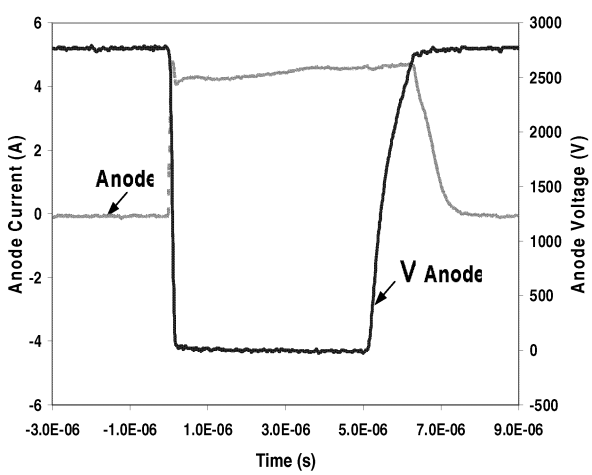

Fig. 9: Expanded view of the Silicon IGBT waveforms.

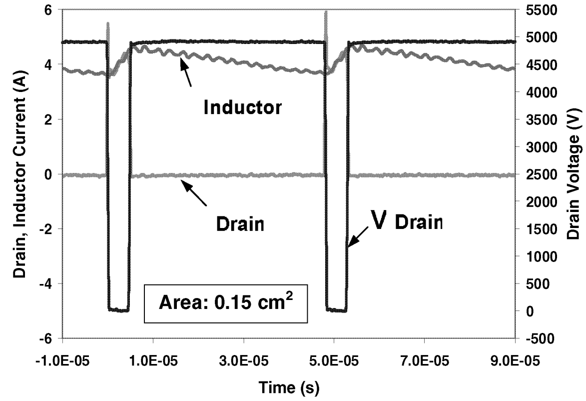

Fig.10: Measured drain voltage, drain current, and inductor current waveforms from the long-term switching stability test using a 10 kV, 5 A SiC MOSFET as Q_{DUT}.

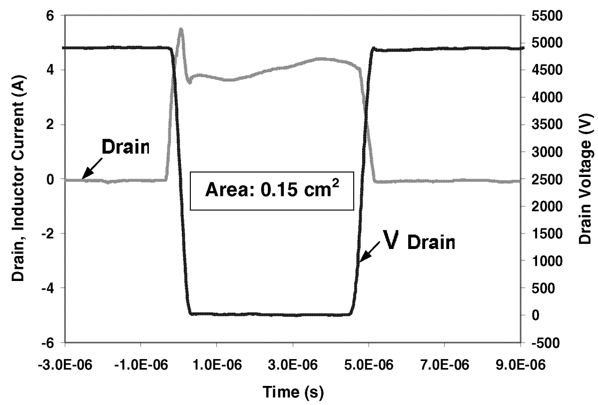

Fig. 11: Expanded view of the SiC MOSFET waveforms.

IV. CONCLUSION

A long-term switching reliability test system for HV-HF SiC power devices was presented. The system uses a 4.5 kV to 5 kV boost converter to emulate the hard switching conditions of a 22.5 kW power converter. An input ground-referenced configuration is used to simplify requirements of the source power supply and power recovery DC-DC converter. A computer graphical user interface was developed to control and monitor the device stability during long-term switching reliability testing. Measured results for a 10 kV, 5 A SiC MOSFET and a 10 kV, 15 kV stacked silicon diodes are compared with the results for a 4.5 kV Silicon IGBT. The results indicate that the SiC MOSFET has higher voltage margin and much faster switching speed.

ACKNOWLEDGEMENT

The work was supported in part by the DARPA WBST HPE Phase 2 program sponsored by Sharon Beermann-Curtin. The authors also wish to acknowledge Jay Huang, a Summer Undergraduate

Research Fellowship (SURF) student for his efforts in helping to develop the control and monitoring software for the test system.

REFERENCES

[1] A. Hefner, "Status of High-Voltage, High-Frequency Silicon-Carbide Power Devices," in *31st GOMACTech Conf.*, pp. 232-235. San Diego, CA, March 2006.

[2] A. Hefner, R. Singh, and J.S. Lai, "Emerging Silicon-Carbide Power Devices Enable Revolutionary Changes in High Voltage Power Conversion," IEEE Power Electronics Society NEWSLETTER, Fourth Quarter 2004, pp. 10-12.

[3] A. Hefner, S-H Ryu, B. Hull, D. Berning, C. Hood, J.M. Ortiz-Rodríguez, A. Rivera-Lopez, T. Duong, A. Akuffo, and M. Hernandez-Mora, "Recent Advances in High-Voltage, High-Frequency Silicon-Carbide Power Devices," in *Recs. 41st IEEE Ind. Apps. Conf.*, Tampa, FL, October 2006.

[4] S. Beerman-Curtin, et al., "Development of SiC High Power Electronics for Naval Aircraft Carriers," in *30th GOMACTech Conf.*, pp. 218-221, Las Vegas, NV, April 2005.

[5]. J.C. Zolper, "Emerging Silicon Carbide Power Electronics Components," IEEE Applied Power Electronics Conference Proceedings, Austin, TX March, 2005.

[6] Sharon Beerman-Curtin, et.al, SiC: The Future of High Power Electronics goamac 06, GOMACTech 2006, pp. 195-197.

[7] Defense Advanced Research Projects Agency (DARPA), Microelectronic Technology Office (MTO), Wide Bandgap Semiconductor Technology High Power Electronics Program (WBG-HPE): http://www.darpa.mil/mto/solicitations/ BAA # 06-30.

[8] R. Singh, Allen R. Hefner, and T. McNutt, "Reliability Concerns in Contemporary SiC Power Devices," Proceedings of the International Semiconductor Device Research.

[9] Vacuum tube triode (6BK4C) datasheet, Tubes website, www.classiccmp.org.

[10] SN74LS221 chip datasheet, On Semiconductors website, www.onsemi.com.

[11] T. H. Duong, A. R. Hefner, and D. W. Berning, "Automated Parameter Extraction Software for High-Voltage, High-Frequency SiC Power MOSFETs," the *10th IEEE* Workshop on Computers in Power Electronics (COMPEL06), July 2006.